

Evaluation of vibro-acoustography techniques to map absorbed dose distribution in irradiated phantoms

Silvio L. Vieira, Randall R. Kinnick, André L. Baggio, Patricia Nicolucci, Mostafa Fatemi, *Senior Member, IEEE*, Adilton O. Carneiro

Abstract— This work presents Vibro-acoustography (VA) as a tool to visualize absorbed dose distributions in a polymer gel dosimeter. VA uses the radiation force of focused ultrasound to vibrate a small region of the sample. Different modalities of VA were used to investigate the feasibility of this technique to evaluate dose distribution in irradiated ‘MAGIC’ polymer gel. A phantom was designed using this polymer with 2% w/w added glass microspheres having an average diameter range between 40–75 μm . The phantom was irradiated using conventional 10 MeV X-rays from a linear accelerator at a distance of 100 cm. An absorbed dose of 50 gray was delivered to the gel. To study the phenomena of dose distribution, continuous wave (CW), toneburst and multifrequency VA were applied to the phantom. Images were generated from the phase and magnitude of the emitted sound from the irradiated area. The comparative accuracy of the different VA results were validated using transverse relaxation rate (R2) image analysis by Magnetic Resonance Imaging (MRI) and a treatment planning system. A contour map of R2 was registered with the transverse CW images, obtained with the focal point on the top surface, and a good correlation was found between the images. The axial profile of irradiated inclusion from the toneburst VA image obtained with excitation frequency of 75 kHz showed the best accuracy compared to other VA modalities. The results show that VA imaging has potential to visualize dose distribution in a polymer gel dosimeter.

I. INTRODUCTION

Vibro-acoustography (VA) uses the radiation force of focused ultrasound to excite a small volume of tissue causing it to vibrate at a frequency Δf . This vibration creates a sound field that can be measured by a nearby hydrophone or microphone. This signal can then be processed to provide quantitative measures of the acoustic emission, such as its amplitude or phase. If the excitation point is raster scanned over a volume, an image of the acoustic emission can be formed. Normally, the radiation force is produced using a two-element confocal transducer with ultrasound beams of two different frequencies, f_0 and $f_0 + \Delta f$, where f_0 is in the

megahertz range and the frequency difference Δf is typically in the kilohertz range. In vibro-acoustography, image information content is intrinsically linked to the value of Δf . To obtain images with different spectral content, multiple scans of the object are necessary. To fully understand a tissue or object’s spectral characteristics, it is desirable to obtain images for different values of Δf .

Two primary methods have been used to induce a force in a focused point into the sample: pulsed (tonebursts) and continuous wave (CW) ultrasound. Both methods use acoustic radiation force produced by focused ultrasonic waves to induce a force into tissue [1-5]. The radiation force can therefore be induced as a static, pulsed, or continuous harmonic force. Short tonebursts with durations of less than 1 ms are typically used to push the tissue. These tonebursts create a transient force, which is assumed to approximate an impulse, at the focus of the beam. The second method employs CW modulated ultrasound wave, which creates a local harmonic vibration at the focal region of the transducer at the modulation frequency [5,6]. The vibrational motion of the sample can then be monitored using acoustic measurements.

Many different types of tissues have been studied using VA, including tissue of the breast [7], arteries [8], and liver [9]. However, in this paper the principle used was based on radiation-induced chemical changes in polymer gel dosimeters, which could be utilized to evaluate absorbed dose distributions [10,11].

The goal of this work is to analyze the different vibro-acoustography modalities used to visualize the absorbed dose distribution in gel. The comparative accuracy of the different modalities in estimating the profile of irradiated region was evaluated.

II. MATERIAL AND METHODS

A. Preparation of gel dosimeter

The gel was prepared using a process similar to that described by [12], followed by the addition of glass microspheres to make a gel dosimeter appropriate for ultrasound evaluation.

Here, the steps to prepare the polymer gel dosimeter (MAGIC gel) are described. First, the gelatin powder (Gelita® South America, Brazil) was added to an Erlenmeyer flask and mixed with the required volume of ultra pure

Manuscript received June 17, 2009. This work was supported in parts by Brazilian agencies of research: CNPq 571801/2008-0, CAPES and FAPESP 2004/14993-2.

S.L. Vieira, A.L. Baggio, P. Nicolucci and A.O. Carneiro (e-mail: adilton@usp.br) are with the Departamento de Física e Matemática, University of São Paulo, Ribeirão Preto, SP, Brazil.

M. Fatemi and R.R. Kinnick are with the Department of Physiology and Biomedical Engineering, Mayo Clinic, Rochester, MN, USA.

deionized water at room temperature. Then the solution was heated to 50°C and stirred continually until total homogeneity was achieved. Afterward, the heat was turned off and the solution was continually stirred until the temperature decreased to 35°C. Then, ascorbic acid (Vetec[®]) and cooper sulfate (Vetec[®]) were added. Five minutes later, methacrylic acid (Acros[®]) and formaldehyde (Acros[®]) were added. After 5 more minutes, 2% of glass microspheres, 40–75 microns, were added to the solution. The solution was continually stirred for 10 more minutes; this agitation was maintained to guarantee homogeneity of the final solution. The polymer gel dosimeter was then transferred to the recipients, which were placed inside a tank of water at 1°C and rotated at 2 rpm for 2 hours.

B. Phantom design

The ‘MAGIC’ gel dosimeter was prepared using only one portion to avoid inter-batch variations. The phantom was made in acrylic cubic block with side length of 8.0 cm. The walls of the block were hermetically sealed using silicone glue to prohibit oxygen diffusion through the gel. Although ‘MAGIC’ gel can produce a suitable dose response when manufactured in normal atmosphere, it has been suggested that its sensitivity can be affected when oxygen diffuses into the post-manufactured gel [10]. The Fig. 1 shows the profile of this phantom placed into the water tank, close to the radiation force transducer and the hydrophone. This configuration was used to perform the VA experiments.

C. Phantom irradiation

The phantom was irradiated using a conventional 10 MeV X-ray radiation therapy unit, Clinac 2300 C/D (Varian Medical Systems, Inc., Mountain View, CA, USA), which was previously calibrated according to the IAEA 398 protocol, yielding an uncertainty smaller than 3% to the dose. The phantom was placed on the isocentre of the linear accelerator unit and was irradiated. Acrylic plates were used to produce a superficial build-up, i.e., maximum dose was delivered at the gel. The phantom was irradiated using 1.0 × 1.0 cm² field size; SSD of 100 cm and an absorbed dose of 50 gray. The irradiated volume was obtained employing parallel-opposed fields (180°) to guarantee dose distribution homogeneity. The Fig. 1 illustrates the irradiated region of the phantom.

D. Virtual planning simulation

The 3D treatment planning system (TPS version 2.07, Medway Technologies Co., Ltd.) was used to simulate the dose distribution from the linear accelerator x-rays into soft tissues. A field-of-view of 13 × 8 cm, with 2.5 cm simulated layer of water bolus in both sides was used to produce a superficial build-up. An antero-posterior irradiation field of 1.0 × 1.0 cm² was employed with x-ray beam energy of 10 MeV. The x-position profile representation of the normalized isodose map is shown in the Fig. 3(a) as a normal distribution (dash line).

E. Relaxation rate acquisition and imaging processing

A calibrated protocol multi-spin-echo sequence (16 echoes) with echo time (TE) multiples of 22.5 ms [22.5 to 360 ms] and long repetition time (TR) of 4,000 ms was used to obtain T2-weighted transversal magnetic resonance images [13]. These images were obtained in a whole-body scanner Magnetom Vision (Siemens, Erlangen, Germany) 1.5 Tesla with a standard head coil. The transverse magnetization relaxation rate (R2) of the water protons was taken as standard measure of the radiation dose absorbed in the ‘MAGIC’ gel dosimeter.

The samples were immersed in a solution containing 99.5% distilled water, 0.2% NaCl and 0.3% MnCl₄–H₂O, to avoid susceptibility artifacts. All measurements were made after the sample had equilibrated to room temperature. The field-of-view was 240 mm and the matrix size (MS) was 256 × 256 pixels, with 4 acquisitions, slice thickness of 3 mm and a signal-to-noise ratio (SNR) of 3.23. An algorithm for mapping R2 based on multiple TE images was developed in MATLAB 7.5 (The Math Works Inc., Natick, MA, USA).

F. Vibro-acoustography experimental setup

The setup used in this experiment was divided in three parts. The first imaging experiment used continuous wave (CW) excitation, the second employed toneburst excitation and the third used multiple CW modulating signals to produce multifrequency radiation force. In all cases, the phantom was positioned transversely and longitudinally as shown in Fig. 1.

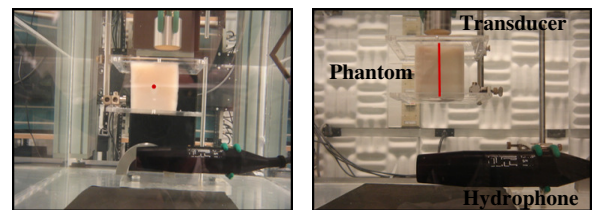


Fig. 1: Experimental setup used. On the left, the block gel positioned with the irradiated area transversally to beam direction and on the right, parallel to beam direction. In both cases, the irradiated area was transversal to the hydrophone.

CW and toneburst procedures made use of a single confocal transducer. This transducer has a focal depth of 70 mm and a center frequency of 3 MHz. The radii of the elements are $a_1 = 14.8$ mm, $a_{21} = 16.8$ mm, and $a_{22} = 22.5$ mm. A two-element confocal ultrasound transducer array was positioned such that the beams met the irradiated volume at their joint focal point. The transducer was moved in steps of 0.2 mm, acquisition matrix 200 × 200 and a field-of-view of 4.0 × 4.0 cm² for all images. Experiments were performed in a large water tank (100 cm × 64 cm × 37 cm) of degassed water. Experiments were conducted in water at room temperature (20° C). The sound produced by the gel vibration was detected by a submerged hydrophone (ITC model 6050, Santa Barbara, CA, USA) with sensitivity –157 dB re 1V/ lPa, and frequency response between 1 Hz and 50

kHz, placed within the water tank (Fig. 1). Because at low frequencies the sound wave propagates almost uniformly in all directions, hydrophone position is not critical. It was kept fixed relatively close to the exposure site but not in the ultrasound path.

1) *Excitation using continuous wave and toneburst:*

In CW and toneburst mode, the confocal elements were driven by two stable radio frequency (RF) synthesizers (HP 33 120A), at frequencies of 3 MHz and 3 MHz + Δf (12.0 to 75 kHz). The Fig. 2(a) shows a VA image performed using this CW modality with modulation frequency of 12.9 kHz.

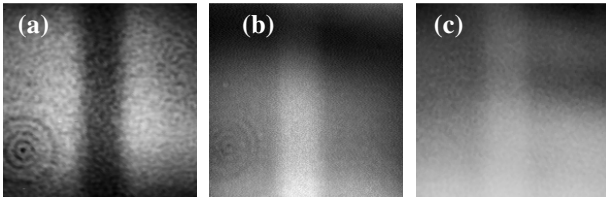


Fig. 2. Shows three modalities of VA image: (a) CW VA magnitude image for 12.9 kHz, (b) toneburst image for 45 kHz and (c) a multifrequency image for 70 kHz of a 50 gray absorbed dose phantom.

The toneburst ultrasound beam was applied using a packet of 300 cycles at 3 MHz signal with time delay of 190 μ s. For this modality, the best image contrast was obtained for larger excitation frequency than one used for CW modality. Fig. 2(b) shows an image obtained for 45 kHz. The received signal was filtered and amplified by a programmable filter (Stanford Research Systems, SR650) to remove noise, then digitized by a 12-bits/sample digitizer (National Instruments VXI-1000) at a rate sufficiently higher (1 or 2 Ms/s) than the Nyquist rate. Data were recorded on a computer disc for later image processing.

2) *Excitation using multifrequency vibration:*

For the multifrequency modality, the radiation stresses at several values of Δf were simultaneously generated and applied to the probe phantom using modulated ultrasound [14,15]. The center elements of the confocal transducer were driven by frequencies $f_{c,1} = 3.025$ MHz and $f_{c,2} = 3.035$ MHz and the annular elements by frequencies $f_{a,1} = 3.075$ MHz, and $f_{a,2} = 3.095$ MHz. The modulated frequencies in the focal region generated from these MHz signals on the central and annular disc were 10, 20, 40, 50, 60, and 70 kHz. The Fig. 2(c) shows an example of VA image of the 50 Gy absorbed dose phantom obtained with this multifrequency modality at 70 kHz.

III. RESULTS AND DISCUSSION

Vibro-acoustography has been shown to have an advantage over other ultrasound techniques in its high displacement sensitivity [4]. As known and demonstrated by several authors, irradiation changes the structure of monomers in the polymer making the volume “stiffer” in comparison to the background gel. Under ultrasound radiation force, the irradiated areas vibrate at the same frequency but with different amplitude than the background.

This vibration creates a sound field that can be measured by a hydrophone. Fig. 2 shows the differing contrasts produced by different frequencies and modalities of radiation force using focused ultrasound.

The accuracy of the estimation of full-width half-maximum (FWHM) of the brightness profiles (transversal line on the VA images) were validated using MRI relaxation rate (R2) and a virtual treatment planning system. Fig. 3 shows the brightness profiles obtained from images of VA and MR techniques and for virtual planning simulation.

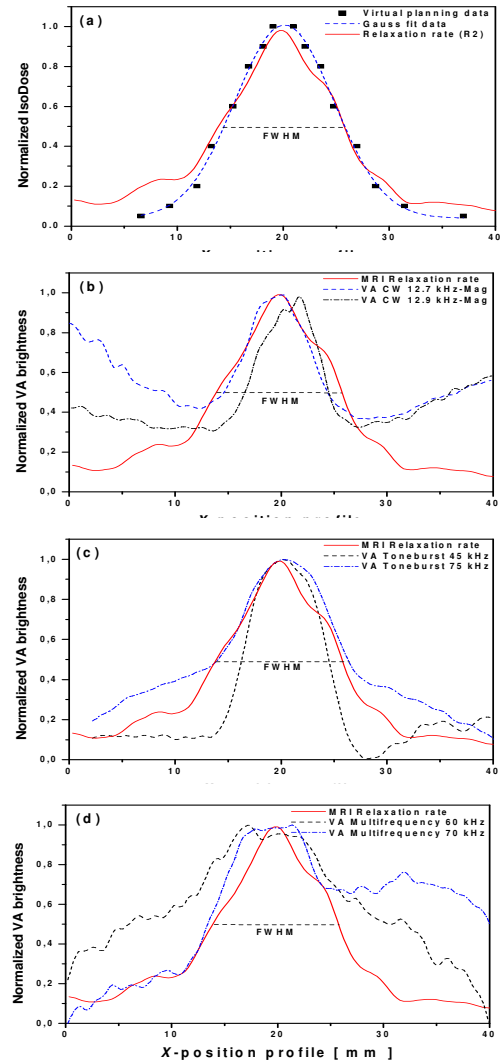


Fig. 3. Set of plots for different VA techniques. In Fig. 3(a) are the x-position profile of the relaxation rate and the planning data fit for the virtual simulation. In (b) is showed the image profile for VA continuous wave. In (c), a set of profiles for VA tonebursts is presented. Finally, in (d) two-multifrequency profile are represented.

Table 1 show the FMHM (extracted from Fig. 3) of these profiles for different techniques, as well the mean difference in contrast between the nonirradiated region and the irradiated one. A signal-to-noise ratio was calculated for the three modalities of Vibro-acoustography images. As shown in Table 1, the toneburst images show the best SNR comparatively. The brightness profile of VA image closest of

TABLE 1

REPRESENTS THE VALUES OF FWHM, DIFFERENCE OF CONTRAST AND SIGNAL-TO-NOISE RATIO FOR VA TECHNIQUES.

Techniques	FWHM (mm)	Difference of contrast	Signal-to-noise (SNR)
Virtual Planning	11.24	–	–
Relaxation Rate	11.83	–	–
Continuous Wave	7.80	83	5.53
Toneburst	12.09	73	12.76
Multi-frequency	> 26	34	10.18

the R2 (11.83 mm) profile was obtained for toneburst modality at 75 kHz (12.09 mm).

Taking these results of FWHM as a tool to estimate the width of the irradiation field, a good concordance is seen with the true irradiation-field size of approximately 10.0 mm. The Fig. 4 shows the R2 isocontour (full lines) registered with the axial CW images.

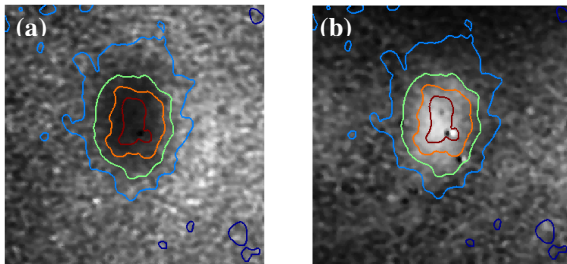


Fig. 4. Transverse CW images obtained with the focal point on the top surface. The magnitude (a) and phase (b) of acoustic emission using $\Delta f = 12.0$ kHz. The R2 isocontour (solid lines) was registered with the VA images.

In the left corner of Fig. 2(a) some dark and light circles are seen. These are artifacts of the imaging process, most likely due to the presence of a gas bubble. The contours with thick solid lines in the Fig. 4 represent regions of the same relaxation rate (R2). The central one is likely related to the high-absorbed dose delivered.

IV. CONCLUSIONS

Experimental Vibro-acoustography images presented in this report have demonstrated the potential of the system in detecting absorbed dose. The vibro-acoustography techniques used had sufficient sensitivity to show the irradiated volume. This volume corresponds approximately to the 8.0 cm^3 region where a 50 gray absorbed dose was delivered. The x -position profile of toneburst vibro-acoustography image with excitation frequency of 75 kHz shows the best accuracy compared to other VA modalities. At the irradiated area, toneburst image technique showed the best signal-to-noise ratios for the highest frequency of modulation.

ACKNOWLEDGMENT

We wish to record our thanks to Dr. James F. Greenleaf for his advice and assistance during this project, and for equipment support to help with these experiments.

REFERENCES

- [1] Sugimoto, T., Ueha, S., and Itoh, K., "Tissue hardness measurement using the radiation force of focused ultrasound" *IEEE Ultrasonics Symposium*, 1377-1380, 1990.
- [2] Fatemi, M., and Greenleaf, J.F., "Ultrasound-stimulated vibro-acoustic spectrography" *Science*, vol. 280, 82-85, Apr. 3, 1998.
- [3] Sarvazyan, A.P., Rudenko, O.V., Swanson, S.D., Fowlkes, J.B., and Emelianov, S.Y., "Shear wave elasticity imaging: a new ultrasonic technology of medical diagnostics" *Ultrasound Med. Biol.*, vol. 24, 1419-35, Nov, 1998.
- [4] Fatemi, M., and Greenleaf, J.F., "Vibro-acoustography: An imaging modality based on ultrasound-stimulated acoustic emission" *Proc. Natl. Acad. Sci. USA*, vol. 96, 6603-8, Jun. 8, 1999.
- [5] Nightingale, K.R., Palmeri, M.L., Nightingale, R.W. and Trahey, G.E., "On the feasibility of remote palpation using acoustic radiation force" *J. Acoustic. Soc. Am.*, vol. 110, 625-34, Jul, 2001.
- [6] Walker, W.F., Fernandez, F.J., and Negron, L.A., "A method of imaging viscoelastic parameters with acoustic radiation force" *Phys. Med. Bio.*, vol. 45, 1437-1447, Jun, 2000.
- [7] Alizad, A., Whaley, D.H. Greenleaf, J.F., Fatemi, M., "Vibro-Acoustography: Identifying breast lesions via a new imaging modality" *RT Image Magazine*, 20(32), 32-34, Aug, 2007.
- [8] Pislaru, C., Kantor, B., Kinnick, R.R., Anderson, J.L, Aubry, M.C., Urban, M.W., Fatemi, M., Greenleaf, J.F., "In Vivo Vibro-acoustography of Large Peripheral Arteries" *Investigative Radiology*, 43(4), 243-252, Apr, 2008.
- [9] Mitri, F.G., Trompette, P. and Chapelon, J.Y., "Improving the use of vibro-acoustography for brachytherapy metal seed imaging: a feasibility study" *IEEE Trans Med Imaging*, vol. 23, 1-6, Jan, 2004.
- [10] Fong, P.M., Keil, D.C., Does, M.D. and Gore, J.C., "Polymer gels for magnetic resonance imaging of radiation dose distributions at normal room atmosphere" *Phys. Med. Biol.* 46 3105-3113, 2001.
- [11] Mather, M.L., DeDeene, Y., Whittaker, A.K., Simon, G., and Baldoek, C., "Investigation of ultrasonic properties of PAG and MAGIC polymer gel dosimeters" *Phys. Med. Biol.* 47(b) 4397-4408, 2002.
- [12] Fernandes, J.P., Pastorello, B.F., Araujo, D.B. and Baffa, O., "Formaldehyde increases MAGIC gel dosimeter melting point and sensitivity" *Phys. Med. Biol.*, 53(4), 53-58, Feb, 2008.
- [13] Carneiro, A.A.O., Vilela, G.R., Araujo, D.B. and Baffa, O., "MRI Relaxometry: Methods and applications" *Brazilian Journal of Physics*, vol. 36, no 1A, Mar, 2006.
- [14] Silva, GT, MW Urban: Image formation of multifrequency vibro-acoustography: Theory and computational simulations. *IEEE 2005, XVII Brazilian Symposium on Computer Graphics and Image Processing*, Natal, Brazil, October 9-12, 2005.
- [15] Urban, M.W., Fatemi, M., Greenleaf, J.F., "Modulated ultrasound and multifrequency radiation force" *Journal of the Acoustical Society of America*, 122, (5 pt 2), 3025, Nov, 2007.